JOC Article

# Ortho Effect in the Bergman Cyclization: Interception of *p*-Benzyne Intermediate by Intramolecular Hydrogen Abstraction

Tarek A. Zeidan, Mariappan Manoharan, and Igor V. Alabugin*

*Department of Chemistry and Biochemistry, Florida State University, Tallahassee, Florida 32306-4390*

*alabugin@chem.fsu.edu*

*Received September 2, 2005*

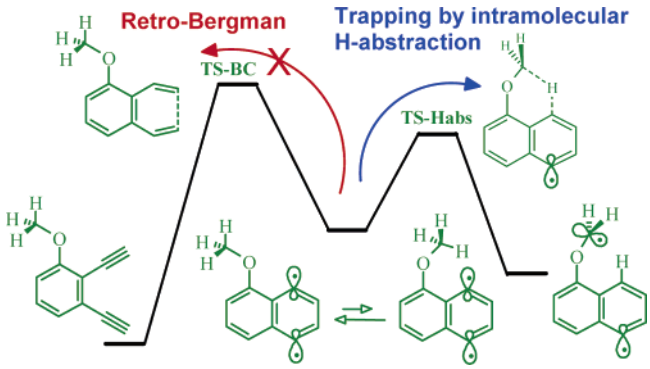


Intramolecular hydrogen atom (H-atom) abstraction from the *o*-$OCH_3$ group effectively intercepts the *p*-benzyne intermediate in the Bergman cycloaromatization of 2,3-diethynyl-1-methoxybenzene (**1**) before this intermediate undergoes either retro-Bergman ring opening or external H-atom abstraction. This process leads to the formation of a new diradical and renders the cyclization step essentially irreversible. Chemical and kinetic consequences of this phenomenon were investigated through the combination of computational and experimental studies.

## Introduction

Control of cycloaromatization reactions through substituent effects provides a promising approach toward practical applications of this chemistry.[1,2] Recently, we reported that the Bergman cyclization of 2,3-diethynyl-1-methoxybenzene (**1**) proceeds faster than the cyclization of 1,2-diethynylbenzene (**2**).[3] Since the computed activation energies for the cyclization of the two enediynes are almost identical, we suggested that this observation may result from trapping of the *p*-benzyne intermediate by intramolecular hydrogen abstraction from the OMe group. In the absence of further facile intramolecular deactivation pathways, such interception of the *p*-benzyne diradical should accelerate the Bergman cyclization by rendering it effectively irreversible, vide infra.[4]

From a chemical perspective, this sequence of steps is interesting because it produces a *new diradical with a different topology and lifetime*. Moreover, since many natural enediyne antibiotics have an OCHR substituent similarly positioned relative to the *p*-benzyne intermediate[5] (Scheme 1), one can speculate that such a "radical relay" mechanism with the concomitant formation of a longer lived diradical may occur in natural antibiotics as well.[6] Because Bergman cyclization is strongly endothermic, the equilibrium between enediyne and *p*-benzyne species is heavily biased toward enediyne, and thus the equilibrium concentration of DNA-damaging species is extremely small. Although this situation may be beneficial for

(1) Maier, M. E.; Greiner, B. *Lieb. Ann. Chem.* **1992**, 855. Schmittel, M.; Kiau, S. *Chem. Lett.* **1995**, 953. Hoffner, J.; Schottelius, M. J.; Feichtinger, D.; Chen, P. *J. Am. Chem. Soc.* **1998**, *120*, 376. Choy, N.; Kim, C. S.; Ballestero, C.; Artigas, L., Diez, C.; Lichtenberger, F.; Shapiro, J.; Russell, K. C. *Tetrahedron Lett.* **2000**, *41*, 6955. Jones, G. B.; Warner, P. M. *J. Am. Chem. Soc.* **2001**, *123*, 2134. König, B.; Pitsch, W.; Klein, M.; Vasold, R.; Prall, M.; Schreiner, P. R. *J. Org. Chem.* **2001**, *66*, 1742. Prall, M. Wittkopp, A.; Fokin, A. A.; Schreiner, P. R. *J. Comput. Chem.* **2001**, *22*, 1605. Alabugin, I. V.; Manoharan, M. *J. Phys. Chem. A* **2003**, *107*, 3363. Alabugin I. V.; Manoharan, M. *J. Am. Chem. Soc.* **2003**, *125*, 4495. Basak, A.; Mandal, S.; Bag, S. S. *Chem. Rev.* **2003**, *103*, 4077. Rawat, D. S.; Zaleski, J. M. *Synlett* **2004**, 393.

(2) Nagata, R.; Yamanaka, H.; Okazaki, E.; Saito, I. *Tetrahedron Lett.* **1989**, *30*, 4995. Myers, A. G, Kuo, E. Y.; Finney, N. S. *J. Am. Chem. Soc.* **1989**, *111*, 8057. Nagata, R.; Yamanaka, H.; Murahashi, E.; Saito, I. *Tetrahedron Lett.* **1990**, *31*, 2907. Myers, A. G.; Dragovich, P. S.; Kuo, E. Y. *J. Am. Chem. Soc.* **1992**, *114*, 9369.

(3) Alabugin, I. V.; Manoharan, M.; Kovalenko, S. V. *Org. Lett.* **2002**, *4*, 1119.

(4) Lockhart, T. P.; Mallon, C. B.; Bergman, R. G. *J. Am. Chem. Soc.* **1980**, *102*, 5976.

10.1021/jo051857n CCC: $33.50 
Published on Web 01/04/2006

**SCHEME 1. Donor C−H Bonds in *p*-Benzynes Derived from OMe Enediyne 1 and from Natural Enediyne Antibiotics**

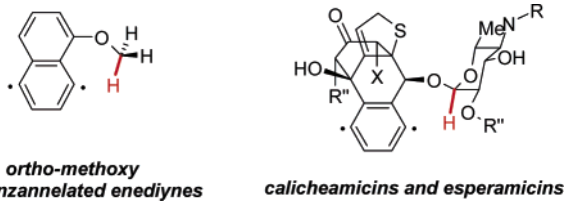


protecting microorganisms that produce enediynes from autodamage, it may also decrease efficiency once the cellular target is reached. Moreover, such internal transformation of a transient radical to a longer lived species based on the above intramolecular H-atom abstraction is interesting because its efficiency should depend on the position of the OCHR moiety, which is, in turn, controlled by molecular environment, e.g., the mode of DNA-binding.[7] Thus, one can envision a scenario where the DNA-binding itself renders the cyclization step irreversible and becomes a necessary condition for the formation of persistent radical species.

The goal of this work is to determine the consequences of this mode of intramolecular H-abstraction through a combination of computational, chemical, and kinetic studies. To achieve this goal, we developed and tested a quantitative kinetic model that extends beyond the Bergman cyclization and incorporates further steps along the cycloaromatization pathway.

## Results and Discussion

The sequence of steps involved in the Bergman cycloaromatization cascade is shown in Scheme 2. Since the cyclization of benzannelated enediynes is significantly endothermic, the barrier for the retro-Bergman ring opening of *p*-benzyne is small ($k_{-1}$ is large).[8] On the other hand, $k_2$ is an order of magnitude smaller in *p*-benzynes than in related phenyl radicals because of the loss of through-bond (TB) interaction in the first hydrogen abstraction step, vide infra.[9]

As a result, the rate of cyclization of benzannelated enediynes *depends on the H-atom donor concentration*,[10] and thus $k_2$ and $k_3$ contribute to the overall kinetic expression. Since H-atom abstraction from 1,4-cyclohexadiene (1,4-CHD) is highly exothermic, formation of either of the three possible monoradicals can be considered irreversible. In the absence of intramolecular H-atom abstraction and other side reactions, the rate of disappearance for the enediyne reactant can be described by eq 1 (derived in Supporting Information):[11]

$$k_{\text{eff}} = k_1 \frac{k_2[\text{HD}]}{k_2[\text{HD}] + k_{-1}} \qquad (1)$$

where rate constants are defined in Scheme 2 and HD stands for H-atom donor. However, when the OMe group is capable of serving as H-atom donor and intercepting the *p*-benzyne radical, the effective rate for the disappearance of OMe enediyne increases and this process becomes less dependent on the "external" H-atom donor concentration. In the extreme case, when $k_3$ is much faster than the rate of intermolecular H-atom abstraction ($k_2[\text{HD}] \ll k_3$), the expression for $k_{\text{eff}}$ becomes *independent of the concentration of* H-atom donor, eq 2:

$$k_{\text{eff}} = \frac{k_1 k_3}{k_{-1} + k_3} \qquad (2)$$

A direct consequence from the above model is that $k_{\text{eff}}$ should be influenced by relative values of $k_2[\text{HD}]$ and $k_{-1}$, providing an explanation to the earlier experimental observations of Semmelhack et al.[10] If $k_{-1}$ (the rate of the retro-Bergman ring opening) is significantly faster in comparison with intermolecular H-atom abstraction by the *p*-benzyne diradical ($k_2[\text{HD}]$), the effective rate for the enediyne disappearance will depend on the concentration of the H-atom donor. In contrast, if the intramolecular H-atom abstraction is fast, effective rate for the disappearance of OMe enediyne should increase and become less dependent on the "external" H-atom donor concentration.

As a first step, we probed the activation and reaction energies for the H-atom abstraction computationally using UBLYP/6-31G** and UB3LYP/6-31G** computations.[12] The six-membered TS for this reaction is 8 and 11 kcal/mol higher than the lowest *p*-benzyne conformer at the two levels of theory, respectively. At both levels, the reaction is exothermic because the newly formed radical center is stabilized by $n(\text{O}) \rightarrow n(\text{C})$ anomeric interaction with the lone pair of the α-oxygen atom. As a result, the new diradical is protected from conversion back to the *p*-benzyne by a ca. 10−15 kcal/mol barrier (Figure 1).[13] Noticeable divergence of the two DFT methods is not surprising due to the known difficulties in describing multiconfigurational electronic structure of singlet biradicals.[14,15] At the higher multiconfigurational BD(T)/cc-pVDZ//BLYP/6-31G** level,[14,16]

(5) *Enediynes Antibiotics as Antitumor Agents*; Doyle, T. W., Borders, D. B., Eds.; Marcel-Dekker: New York, 1994. Esperamicin: Golik, J.; Clardy, J.; Dubay, G.; Groenewold, G.; Kawaguchi, H.; Konishi, M.; Krishnan, B.; Ohkum, H.; Saitoh, K.; Doyle, T. W. *J. Am. Chem. Soc.* **1987**, *109*, 3461. Golik, J.; Dubay, G.; Groenewold, G.; Kawaguchi, H.; Konishi, M.; Krishnan, B.; Ohkum, H.; Saitoh, K.; Doyle, T. W. *J. Am. Chem. Soc.* **1987**, *109*, 3462. Calicheamicin: Lee, M. D.; Dunne, T. S.; Siegel, M. M.; Chang, C. C.; Morton, G. O.; Borders, D. B. *J. Am. Chem. Soc.* **1987**, *109*, 3464. Lee, M. D.; Dunne, T. S.; Chang, C. C.; Ellestad G. A.; Siegel, M. M.; Morton, G. O.; McGahren, W. J.; Borders, D. B. *J. Am. Chem. Soc.* **1987**, *109*, 3466.

(6) Interestingly, interaction of esperamicin A with CT-DNA results in cleavage of the glycosidic bond connecting the sugar to the warhead. Although hydrogen abstraction at the anomeric carbon has been suggested as a possible explanation to this process, the exact mechanism by which the cleavage of the C−O bond occurs is still unknown. Langley, D. R.; Golik, J.; Krishnan, B.; Doyle, T. W.; Beveridge, D. L. *J. Am. Chem. Soc.* **1994**, *116*, 15.

(7) Uesugi, M.; Sugiura, Y. *Biochemistry* **1993**, *32*, 4622. Walker, S.; Murnick, J.; Kahne, D. *J. Am. Chem. Soc.* **1993**, *115*, 7954. Ikemoto, N.; Kumar, R. A.; Dedon, P. C.; Danishefsky, S. J.; Patel, D. J. *J. Am. Chem. Soc.* **1994**, *116*, 9387. Paloma, L. G.; Smith, J. A.; Chazin, W. J.; Nicolaou, K. C. *J. Am. Chem. Soc.* **1994**, *116*, 3697. Kumar, R. A.; Ikemoto, N.; Patel, D. J. *J. Mol. Biol.* **1997**, *265*, 187.

(8) Decrease in retro-Bergman barrier for benzannelated enediynes: Haberhauer, G.; Gleiter, R. *J. Am. Chem. Soc.* **1999**, *121*, 4664. Koseki, S.; Fujimura, Y.; Hirama, M. *J. Phys. Chem.* **1999**, *103*, 7672.

(9) Logan, C. F.; Chen, P. *J. Am. Chem. Soc.* **1996**, *118*, 2113. Schottelius, M. J.; Chen, P. *J. Am. Chem. Soc.* **1996**, *118*, 4896.

(10) Semmelhack, M. F.; Neu, T.; Foubelo, F. *J. Org. Chem.* **1994**, *59*, 5038. Kaneko, T.; Takahashi, M.; Hirama, M. *Tetrahedron Lett.* **1999**, *40*, 2015. For a recent discussion, see: Semmelhack, M. F., Sarpong, R. *J. Phys. Org. Chem.* **2004**, *17*, 807.

(11) See Supporting Information for a more elaborate kinetic analysis including the presence of competing reactions and formation of byproducts.

(12) Frisch, M. J. et al. *Gaussian 98*, revision A.9; Gaussian, Inc.: Pittsburgh, PA, 1998 (see Supporting Information for full citation).

(13) This is reminiscent of the Myers−Saito cyclization where the benzylic radical orbital undergoes rotation to achieve coplanarity with the π-system of the benzene ring after the cyclization TS. The additional stabilization of the product makes this reaction effectively irreversible: Engels, B.; Hanrath, M. *J. Am. Chem. Soc.* **1998**, *120*, 6356.

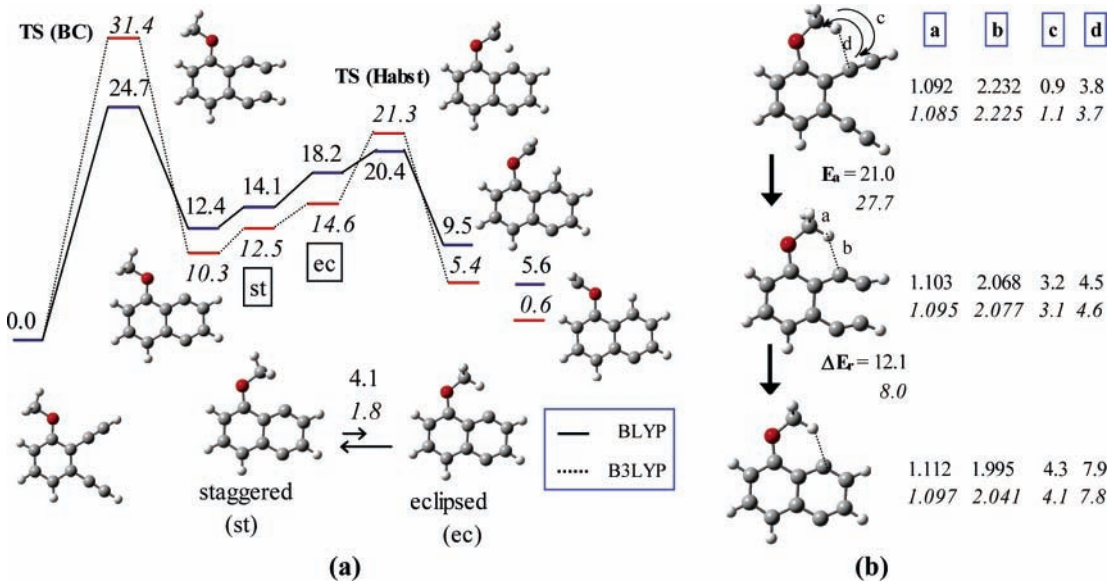


**FIGURE 1.** (a) Computational analysis of Bergman cyclization/intramolecular H-atom abstraction cascade of 2,3-diethynyl-1-methoxybenzene (**1**) at the BS-UBLYP/6-31G** and UB3LYP/6-31G** levels (in italics). (b) Structural information for the Bergman cyclization of *syn*-OMe (ec): "a" and "b" denote the C−H distances in Å and "c" and "d" correspond to the energies of $\sigma(CH) \rightarrow \pi^*(CC)_i$ and $\pi(CC)_{inplane} \rightarrow \sigma^*(CH)$ interactions, respectively. All energies are in kcal/mol.

**SCHEME 2. Kinetic Model for the Bergman Cyclization of 2,3-Diethynyl-1-methoxybenzene (1)**

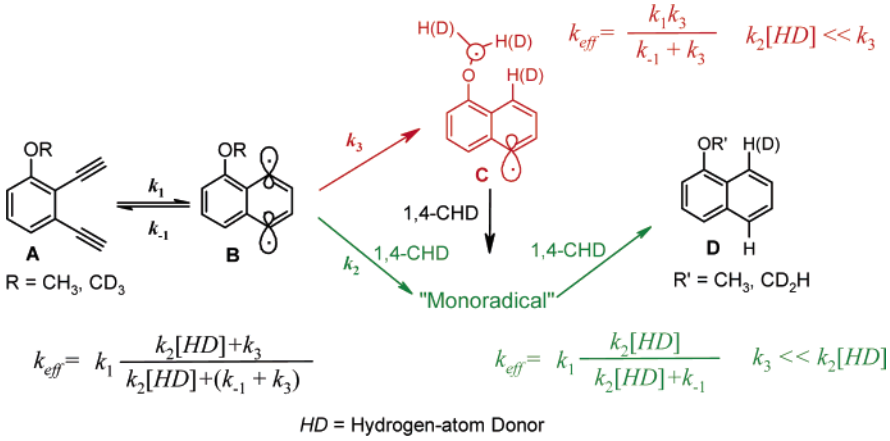


the activation energy for the Bergman cyclization is 28.8 kcal/mol and that for the H-abstraction is 6.2 kcal/mol. Both of the BD(T) barriers lie between the respective BLYP and B3LYP values. To obtain more reliable computational data, we carried out analogous calculations in monoradical where complications due to the multiconfigurational nature of wave functions are not present and where MP2/631-G** computations can be used to cross-evaluate performance of the two DFT methods (Figure 2). Although the calculated barriers for intramolecular H-abstraction in the monoradical vary from 4.8 to 7.7 kcal/mol,[17] these variations do not change the general conclusion that intramolecular H-abstraction should be able to compete efficiently with the retro-Bergman ring opening.

Interestingly, the cyclization of the eclipsed *syn*-conformer of the OMe-enediyne is accompanied by noticeable weakening of the C−H bond. This weakening resembles that in the Schmitel cyclization/H-abstraction sequence (formal ene reac-

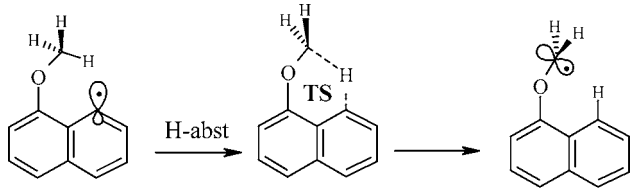


| | $E_a$ | $\Delta E_r$ |
|---|---|---|
| UB3LYP/6-31G** | 6.4 | -9.6 |
| UBLYP/6-31G** | 4.8 | -9.5 |
| UMP2/6-31G** | 7.7 | -14.3 |

**FIGURE 2.** Calculated energies for intramolecular H-abstraction from the OMe-monoradical.

(14) Kraka, E.; Cremer, D. *J. Am. Chem. Soc.* **2000**, *122*, 8245 and references therein. For the most recent discussion of the theoretical methods, see: Schreiner, P. R.; Navarro-Vazquez, A.; Prall, M. *Acc. Chem. Res.* **2005**, *38*, 29.

(15) A recent example: Alabugin, I. V.; Manoharan, M. *J. Am. Chem. Soc.* **2005**, 12583.

(16) (a) Cramer, C. J. *J. Am. Chem. Soc.* **1998**, *120*, 6261. (b) Prall, M.; Wittkopp, A.; Schreiner, P. R. *J. Phys. Chem. A* **2001**, *105*, 9265. (c) Crawford, T. D.; Kraka, E.; Stanton, J. F.; Cremer, D. *J. Chem. Phys.* **2001**, *114*, 10638. (d) Stahl, F.; Moran, D.; Schleyer, P. v. R.; Prall, M.; Schreiner, P. R. *J. Org. Chem.* **2002**, *67*, 1453.

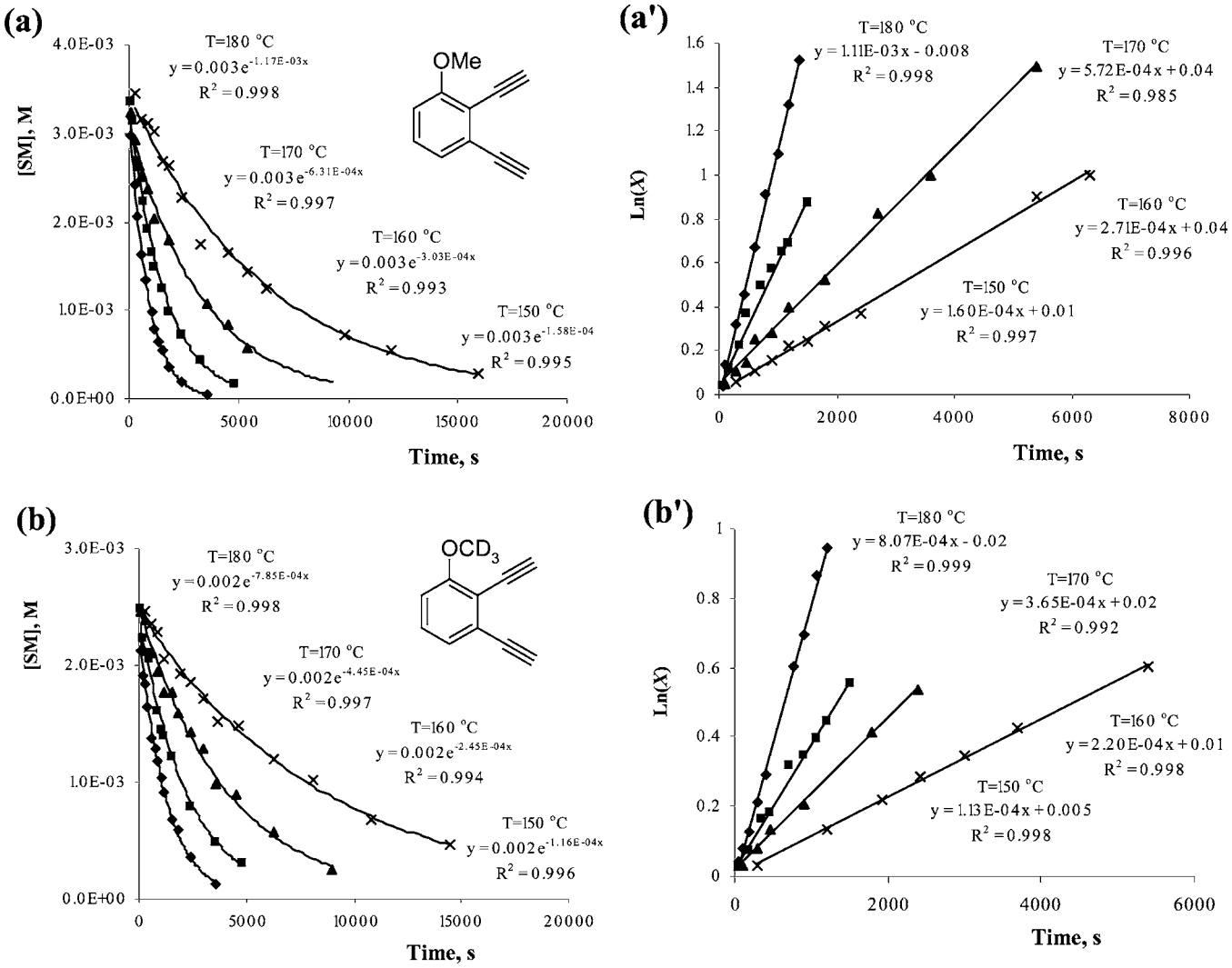


**FIGURE 3.** Pseudo-first-order rate constants determined using GC analysis for the disappearance of enediynes (a) 2,3-diethynyl-1-methoxybenzene (**1**) ($3.33 \times 10^{-3}$ M) and (b) 2,3-diethynyl-1-trideuteriomethoxybenzene (**3**) ($2.5 \times 10^{-3}$ M) and the appearance of corresponding naphthalenes (a′) 1-methoxynaphthalene and (b′) 1-methoxy($OCD_3$)naphthalene at different temperatures; [1,4-CHD] = 0.3 M; *X* is defined in eq 4.

tion) of enyne-allenes analyzed recently by Lipton, Singleton, and co-workers,[18] but the sequence of cyclization and hydrogen transfer steps in our case is far from being concerted.

To test validity of the computational estimates, we compared reaction rates and activation energies for the 2,3-diethynyl-1-methoxybenzene (**1**), its $OCD_3$ analogue (**3**), and 1,2-diethynylbenzene (**2**)[19] using several experimental approaches: (a) differential scanning calorimetry (DSC) of neat samples and solutions in 1,4-cyclohexadiene (1,4-CHD) and (b) kinetic analysis under the pseudo-first-order conditions (Figure 3 and Table 1). Although the activation energies for the disappearance of the three enediynes and for the formation of corresponding naphthalene products are within experimental error, the DSC barrier determined in 1,4-CHD is higher for the deuterated enediyne and consumption of 2,3-diethynyl-1-methoxybenzene proceeds on average 1.4-fold faster than that of 2,3-diethynyl-1-trideuteriomethoxybenzene (**3**) at this concentration of 1,4-CHD, vide infra. This observation can be explained by the deuterium isotope effect on the intramolecular hydrogen abstraction step displayed indirectly as described in eq 2.

Apparent or effective rate constants, $k_{eff}$, were determined using the method described in the Experimental Section. Effective rate constants for the disappearance of *ortho*-substituted enediynes and appearance of the corresponding naphthalene products were measured at different temperatures. Consumption of enediynes followed the pseudo-first-order exponential decay dependence (eq 3), Figure 3a and b:

$$[\mathrm{SM}] = [\mathrm{SM}]_0\, e^{-k_{eff}t} \qquad (3)$$

where $[SM]_0$ is the initial concentration of enediyne, [SM] is

(17) Based on the loss of through bond (TB) interaction between the two radical centers, reactions of diradicals should have slightly higher barriers than analogous reactions of monoradicals. For example, Chen found that for *p*-benzyne at the CASPT2N/6-31G**//CAS/3-21G level the difference in the barriers of first and second H-abstractions from methanol is ca. 1.6 kcal/mol. This observation suggests that UB3LYP provides a more reliable description of these reactions than UBLYP. For more detailed description of TB interactions, see: Hoffmann, R.; Imamura, A.; Hehre, W. J. *J. Am. Chem. Soc*. **1968**, *90*, 1499. Hoffmann, R. *Acc. Chem. Res.* **1971**, *4*, 1. Squires, R. R.; Cramer, C. J. *J. Phys. Chem. A* **1998**, *102*, 9072. Theoretical analysis of TB interaction in cations: Alabugin I. V.; Manoharan, M. *J. Org. Chem.* **2004**, *69*, 9011.

(18) Bekele, T.; Christian, C. F.; Lipton, M. A.; Singleton, D. A. *J. Am. Chem. Soc.* **2005**, *127*, 9216.

(19) Our results are in excellent agreement with previously reported values: Grissom, J. W.; Calkins, T. L.; McMillen, H. A.; Jiang, Y. H. *J. Org. Chem.* **1994**, *59*, 5833.

**TABLE 1. Comparison of Activation Energies and Preexponential Factors (log *A*) Determined with Different Techniques and Yields of 1-Substituted Naphthalenes[a]**

| | activation energies, kcal/mol | | | | preexponential factor, log *A* ($s^{-1}$) | | | |
|---|---|---|---|---|---|---|---|---|
| ene-diyne | BLYP (B3LYP)[b] | DSC[c] | disappearance of ED | appearance of naphthalene | DSC[c] | disappearance of ED | appearance of naphthalene | % yield[d] |
| 1 | 24.7 (31.4) | 23.2 ± 0.2 (22.1 ± 0.5) | 25.5 ± 0.6 | 24.9 ± 1.4 | 10.1 ± 0.2 (11.3 ± 0.5) | 9.4 ± 0.3 | 9.0 ± 0.7 | 65 |
| 3 | 24.8 (31.3)[e] | 24.3 ± 0.2 (22.1 ± 0.7) | 24.2 ± 0.8 | 24.4 ± 1.6 | 10.6 ± 0.2 (11.3 ± 0.7) | 8.6 ± 0.4 | 8.6 ± 0.8 | 62 |
| 2 | 24.5 (31.3) | 23.1 ± 0.1 (21.7 ± 0.3) | 25.9 ± 1.1[f] | 26.0 ± 1.5 | 10.0 ± 0.1 (10.8 ± 0.3) | 9.4 ± 0.6 | 9.4 ± 0.8 | 35 |

[a] Errors are standard deviations with 90% confidence limits. [b] Staggered *anti* conformer for $OCH_3$; 6-31G** basis set[3] (see also Supporting Information). [c] In neat 1,4-CHD, using ASTM E-698 thermal stability procedure; values in parentheses are for neat enediynes. [d] Determined by GC. [e] The isotope calculations have been done at 298 K and 1 atm. [f] This value is in good agreement with the earlier report of Grissom et al.[19]

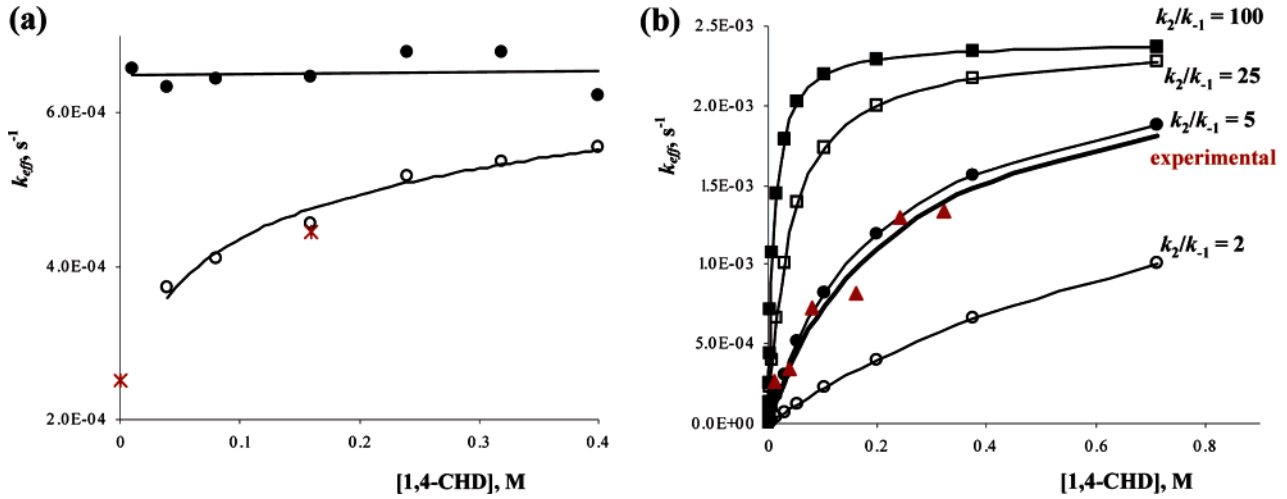


**FIGURE 4.** Dependence of the effective rate constant on the 1,4-CHD concentration for (a) the consumption of 2,3-diethynyl-1-methoxybenzene (**1**) (filled circles) and 2,3-diethynyl-1-trideuteriomethoxybenzene (**3**) (red crosses) and formation of 1-methoxynaphthalene (open circles) at 170 °C and (b) trends in $k_{eff}$ at different $k_{-1}$:$k_2$ ratios predicted by eq 1 when $k_1 = 2.4 \times 10^{-3}$ M vs the experimental dependence of the rate of consumption for 1,2-diethynylbenzene (**2**) solution ($3.9 \times 10^{-3}$ M) at 188 °C, shown in red triangles. At infinite concentration of 1,4-CHD the apparent rate constant will approach asymptotically the value of $k_1 = 2.4 \times 10^{-3}$ M.

the concentration of enediyne at time *t*, and $k_{eff}$ is the effective rate concentration of the reaction.

Similarly, the appearance of naphthalene products followed pseudo-first-order kinetic behavior, Figure 3a′ and b′. The effective rate constants, $k_{eff}$, for the formation of the Bergman products were determined by fitting the data to eq 4, which normalizes formation of the product to the observed reaction yield:

$$\ln(X) = \ln\left(\frac{[P]_{inf}}{[P]_{inf} - [P]}\right) = k_{eff}t \qquad (4)$$

where [P] and $[P]_{inf}$ are concentrations of the corresponding naphthalene product at time *t* and infinity, respectively, and $k_{eff}$ is the effective rate constant for the appearance of the Bergman product. Activation energies and preexponential factors were determined by fitting the effective rate constants at different temperatures to the Arrhenius plot. The results are given in Table 1.

The key evidence for the intramolecular *p*-benzyne interception is provided by the response of experimental reaction rates to variations in the H-atom concentration. The experimentally measured trend in Figure 4a clearly follows eq 2, where the consumption of 2,3-diethynyl-1-methoxybenzene (**1**) is independent from the concentration of the *external* hydrogen donor, 1,4-CHD. As a result, the Bergman cycloaromatization step in this case can be considered *irreversible*, with the *p*-benzyne intermediate being funneled down the reaction path and the retro-Bergman step effectively shut-off. On the other hand, formation of 1-methoxynaphthalene requires the presence of a H-atom donor, and thus the respective effective rate constant is dependent on the concentration of 1,4-CHD (Figure 4a).

In contrast, the rate of consumption of 1,2-diethynylbenzene (**2**) depends on 1,4-CHD concentration.[8,10] Comparison of the experimental curve with theoretical predictions at different $k_2/k_{-1}$ ratios based on eq 1 suggests that the ratio of experimental rate constants for H-atom abstraction and retro-Bergman reaction is ca. 5 $M^{-1}$ (Figure 4b). An important consequence from the dependence of experimental curves from the $k_2/k_{-1}$ ratios is that only the absolute concentration of H-donor is important, whereas the excess of H-donor relative to enediyne is not. For instance, experiments with 100-fold excess of 1,4-CHD relative to 1 mM and 0.01 mM concentration ratio of enediyne are not comparable. Since the 1,4-CHD excess per se is irrelevant, we suggest that only the *absolute* concentrations of H-donors should be reported in kinetic studies of Bergman cyclization and related reactions. Moreover, since $k_2/k_{-1}$ ratios are different for different enediynes, the pseudo-first-order plateau will be reached at different 1,4-CHD concentrations. Thus, kinetic studies relying on the pseudo-first-order approximations should carefully examine the effect of H-atom concentration for each new substrate.[20]

Both the intramolecular hydrogen abstraction and the relatively long lifetime of the intermediate α-aryloxy radical are

further supported by formation of the product of the cyclohexadienyl radical recombination with $OCH_2$ moiety derived from the methoxy group (see Supporting Information, Figure S1c). Finally, we observed D-incorporation at the C8 of the naphthalene ring with the concomitant H-incorporation at the methoxy group in the $OCD_3$ substrate. The $^1$H NMR signal of the methoxy moiety in the naphthalene product derived from the deuterated anisole **3** (see Supporting Information, Figure S1b) is a quintet at 3.9 ppm due to proton coupling with the two deuterium atoms in the $OCHD_2$ moiety. Furthermore, the integral intensity (0.8) of the proton at C8 in 1-methoxynaphthalene is decreased in proportion to the intensity of the $OCHD_2$ signal. The extent of D-incorporation provides an insight into the relative rates of intramolecular and intermolecular H-atom abstraction. At the 0.33 M concentration of 1,4-CHD, about 20% of D is transferred, indicating the $k_2$[CHD]/$k_3$ ratio of 4:1 (see Supporting Information, Figure S1b).

Although direct determination of the extent of D-incorporation at lower concentration of 1,4-CHD is complicated by low yields of naphthalene products under these conditions, these data suggest the dominance of the intramolecular H-atom transfer (>96%) at equal concentrations (0.0033 M) of the enediyne and the H-atom donor when $k_2$[CHD]/$k_3$ ratio is as low as 0.04:1. Most interestingly, these observations also suggest that the D-effect on $k_3$ is significant and intramolecular interception becomes less competitive with H-abstraction from the external donor and retro-Bergman ring opening. Indeed, the rate of disappearance of $OCD_3$-labeled enediyne (red crosses in Figure 3a) becomes sensitive to [1,4-CHD] concentration.

## Conclusion

In conclusion, the OMe group in 2,3-diethynyl-1-methoxybenzene (**1**) intercepts the *p*-benzyne diradical through intramolecular H-atom abstraction. This step renders cyclization effectively irreversible and provides a route to diradicals with new topologies that are likely to be longer living than *p*-benzyne. The question of whether the same mechanism operates in calicheamicins and esperamicins as well as further implications for DNA damage and triggering of cascade radical reactions[21] are under investigation.

## Experimental Section

2-Iodo-3-nitrophenol[22] and 2,3-diethynyl-1-methoxybenzene (**1**)[3] were prepared according to literature procedures. Capillaries (300 mm length, 1.5−1.8 mm outer diameter, 0.2 mm wall) used in kinetic studies were purchased from Freidrick and Dimmock Inc.

**Synthetic Procedures. Synthesis of 2-Iodo-1-trideuteriomethoxy-3-nitrobenzene (4).** KOH pellets (0.11 g, 1.96 mmol) were added to a solution of 2-iodo-3-nitrophenol (0.50 g, 1.89 mmol) in MeOH (10 mL) and stirred for 20 h. The red precipitate of potassium 2-iodo-3-nitrophenolate (0.50 g, 1.65 mmol) was filtered, dissolved in dry acetonitrile, and placed in an Ace pressure tube. $CD_3I$ was added and the reaction was heated to 80 °C for 30 min. After the reaction mixture turned yellow, the solvent was evaporated under vacuo. The residue was dissolved in $CH_2Cl_2$, washed with $H_2O$ (2 × 20 mL), and dried over $Na_2SO_4$. The solvent was removed under vacuum. Recrystallization from hexanes afforded 0.45 g (85%) of the desired product as yellow crystals: mp 93−95 °C; $^1$H NMR (300 MHz, $CDCl_3$) $\delta$ 7.4 (dd, 1H, $J$ = 8.4, 7.8 Hz), 7.3 (dd, 1H, $J$ = 8.4, 1.2 Hz), 6.9 (dd, 1H, $J$ = 8.1, 1.2 Hz); $^{13}$C NMR (75.5 MHz, $CDCl_3$) $\delta$ 159.7, 155.7, 130.0, 119.8, 113.4, 79.9; UV−vis ($CH_3CN$) $\lambda_{max}$ (lg $\epsilon$) = 317 nm (3.81), 272 (3.46), 222 (4.13); IR (neat) 3074, 1522, 1448, 1348, 1285, 1098 cm$^{-1}$; HRMS (EI+) calcd for $C_7H_3D_3NO_3I$ 281.95810, found 281.95873.

**Synthesis of 2-Iodo-3-trideuteriomethoxy-1-aminobenzene (5).** $SnCl_2$ (2.5 g, 12.9 mmol) was added to 2-iodo-1-trideuteriomethoxy-3-nitrobenzene (**4**) (0.73 g, 2.59 mmol) in 5 mL of EtOH. The reaction was stirred at room temperature for 32 h. The solvent was evaporated under vacuum and the residue was rendered alkaline by adding NaOH (1N). The mixture was extracted with $CH_2Cl_2$ (3 × 10 mL) and the organic mixture was washed with $H_2O$ (2 × 10 mL) and dried over $Na_2SO_4$. The solvent was removed under vacuum. The reaction mixture was purified by chromatography on silica gel (hexanes) to afford 0.49 g (75%) of the desired product as a yellow solid: mp 42 °C; $^1$H NMR (300 MHz, $CDCl_3$) $\delta$ 7.08 (d, 1H, $J$ = 8.1, 7.8 Hz), 6.39 (dd, 1H, $J$ = 8.1, 1.2 Hz), 6.20 (dd, 1H, $J$ = 8.1, 1.2 Hz), 4.25 (bs, 2H); $^{13}$C NMR (75.5 MHz, $CDCl_3$) $\delta$ 185.8, 148.4, 129.6, 107.8, 100.4, 75.8, 55.4 (septet, $J$ = 21.7 Hz); UV−vis ($CH_3CN$) $\lambda_{max}$ (lg $\epsilon$) = 293 nm (3.36), 238 (3.93), 214 (4.54); IR (neat) 3348, 1608, 1454, 1266, 1101, 761 cm$^{-1}$; HRMS (EI+) calcd for $C_7H_5D_3NOI$ 251.98392, found 251.98476.

**Synthesis of 2,3-Diiodo-1-trideuteriomethoxybenzene (6).** Dropwise addition of a solution of sodium nitrite (0.21 g, 3.06 mmol) in 6 mL of water to a solution of 2-iodo-3-deuteriomethoxy-1-aminobenzene (**5**) (0.70 g, 2.78 mmol) in 11 mL of HCl (prepared from 5 mL of concentrated HCl and 6 mL of $H_2O$ solution) at 5 °C was carried out over 30 min. After the mixture was stirred for additional 20 min at 5 °C, a solution of potassium iodide (3.1 g, 19.2 mmol) in $H_2O$ (4 mL) was added dropwise. The solution was then heated at 80 °C for 2 h, cooled, and extracted with $CH_2Cl_2$ (3 × 10 mL). The combined extracts were washed with 5% aqueous sodium bisulfite and dried over $Na_2SO_4$. The solvent was removed under vacuum. The reaction mixture was purified by chromatography on silica gel (hexanes) to afford 0.71 g (70%) of the desired product as a white solid: mp 71−72 °C; $^1$H NMR (300 MHz, $CDCl_3$) $\delta$ 7.5 (d, 1H, $J$ = 8.1, 1.5 Hz), 7.0 (dd, 1H, $J$ = 8.1, 8.1 Hz), 6.7 (d, 1H, $J$ = 7.2 Hz); $^{13}$C NMR (75.5 MHz, $CDCl_3$) $\delta$ 159.8, 131.7, 130.5, 109.7, 109.4, 100.4; UV−vis ($CH_3CN$) $\lambda_{max}$ (lg $\epsilon$) = 291 nm (3.36), 283 (3.43), 217 (4.40); IR (neat) 3054, 2255, 2228, 2068, 1558, 1335, 1267, 1102, 989, 764 cm$^{-1}$; HRMS (EI+) calcd for $C_7H_3D_3OI_2$ 362.86970, found 362.86909.

**Synthesis of 2,3-Bis(trimethylsilylethynyl)-1-trideuteriomethoxybenzene (7).** A suspension of 2,3-diiodo-1-trideuteriomethoxybenzene (**6**) (2.10 g, 5.78 mmol), $PdCl_2(PPh_3)_2$ (203 mg, 0.29 mmol), and Cu(I) iodide (55.0 mg, 0.29 mmol) in 40 mL of $(i\text{-Pr})_2NH$ was degassed three times by the freeze/pump/thaw technique in a flame-dried screw-cap Ace pressure tube. Trimethylsilyl (TMS) acetylene (1.36 g, 13.8 mmol) was added using a syringe. The tube was sealed and the mixture was heated at 100 °C for 3 h in an oil bath. Reaction was monitored by TLC. After total consumption of the aryl halide, the reaction mixture was filtered through Celite and washed with methylene chloride (3 × 30 mL). The organic layer was washed with a saturated solution of ammonium chloride (2 × 30 mL) and water (2 × 30 mL) and dried over anhydrous $Na_2SO_4$. Solvent was removed under vacuum. The reaction mixture was purified by flash chromatography on silica gel (hexanes) to afford 1.40 g (80%) of the desired product as yellow needles: mp 65 °C; $^1$H NMR (300 MHz, $CDCl_3$) $\delta$ 7.12 (dd, 1H, $J$ = 8.1, 7.8 Hz), 7.04 (d, 1H, $J$ = 7.8 Hz), 6.74 (d, 1H, $J$ = 8.2 Hz), 0.27 (s, 9H), 0.25 (s, 9H); $^{13}$C NMR (75.5 MHz, $CDCl_3$) $\delta$ 160.2, 128.9, 127.7, 124.5, 114.9 110.6, 103.1, 102.8,

(20) A thorough kinetic study on the effect of H-atom donor for different *ortho*-substituted benzannelated enediynes is described in a separate manuscript: Zeidan, T. A.; Kovalenko, S. V.; Manoharan, M.; Alabugin, I. V. *J. Org. Chem.* In press.

(21) Although intramolecular trapping of *p*-benzynes by reactions with $\pi$-bonds is known (Grissom, J. W.; Calkins, T. L. *J. Org. Chem.* **1993**, *58*, 5422; Grissom, J. W.; Calkins, T. L.; Egan, M. *J. Am. Chem. Soc.* **1993**, *115*, 11744), its atom transfer counterpart is virtually unexplored.

(22) Hine, J.; Hahn, S.; Miles, D. E.; Ahn, K. *J. Org. Chem.* **1985**, *50*, 5092.

99.2, 89.1, −0.2, −0.3; UV−vis ($CH_3CN$) $\lambda_{max}$ (lg $\epsilon$) = 328 nm (3.14), 315 (3.10), 283 (3.98), 243 (4.44); IR (neat) 2960, 2156, 1562, 1460, 1249, 1110, 844, 760 $cm^{-1}$; HRMS (EI+) calcd for $C_{17}H_{21}D_3OSi_2$ 303.15541, found 303.15549.

**Synthesis of 2,3-Diethynyl-1-trideuteriomethoxybenzene (3).** NaOH (1 N, 5 mL) was added to a methanol solution (50 mL) of 2,3-bis(trimethylsilylethynyl)-1-trideuteriomethoxybenzene (**7**) (1.10 g, 3.63 mmol). The mixture was stirred at room temperature for 15 min. The progress of reaction was monitored by TLC. After total consumption of the TMS acetylenes, the solvent was removed in vacuo. Aqueous HCl (1 N, 10 mL) was added to the crude mixture. The acidic mixture was extracted by dichloromethane (3 × 20 mL). The organic layer was washed with water (2 × 30 mL) and dried over anhydrous $Na_2SO_4$. Solvent was removed under vacuum. The reaction mixture was purified by flash chromatography on silica gel (hexanes) to afford 0.50 g (86%) of the desired product as a white solid: mp 52 °C; $^1$H NMR (300 MHz, $CDCl_3$) $\delta$ 7.2 (dd, 1H, $J$ = 8.1, 7.8 Hz), 7.1 (d, 1H, $J$ = 7.5 Hz), 6.8 (dd, 1H, $J$ = 9.3), 3.6 (s, 1H), 3.3 (s, 1H); $^{13}$C NMR (75.5 MHz, $CDCl_3$) $\delta$ 160.6, 129.4, 126.5, 124.6, 113.9, 110.9, 85.4, 81.6, 81.2, 78.0, 55 (septet, $J$ = 22.3 Hz); UV−vis ($CH_3CN$) $\lambda_{max}$ (lg $\epsilon$) = 321 nm (3.61), 267 (3.99), 258 (3.94), 254 (3.93), 235 (4.57); IR (neat) 3280, 2230, 2073, 1565, 1458, 1294, 1104, 789, 633 $cm^{-1}$; HRMS (EI+) calcd for $C_{11}H_5D_3O$ 159.07635, found 159.07608.

**Representative Procedure for Preparative Scale of Bergman Cyclizations.** 2,3-Diethynyl-1-methoxybenzene (**1**) (75 mg, 0.48 mmol) was dissolved in anhydrous chlorobenzene (9 mL). 1,4-Cyclohexadiene (4.5 mL, 48 mmol) was added and the mixture was placed in a Pyrex glass tube equipped with a joint. The tube was attached through the joint to a vacuum line and the mixture was degassed three times by the freeze/pump/thaw technique. The tube was sealed under argon, placed in an oil bath, and heated to 150 °C for 5 h. After cooling, chlorobenzene was distilled under vacuum and the products were isolated and purified by HPLC using hexanes HPLC grade as solvent with 4 mL/min flow rate, 265 nm detection wavelength, and 500 $\mu$L loop.

**Differential Scanning Calorimetry Studies.** Temperature and enthalpy calibrations were performed using indium standard. The heat capacity was calibrated using a 25 mg sapphire standard. About 8−10 mg of enediyne was used for each experiment. For neat samples, enediynes were sealed in aluminum hermetic pans. The samples were equilibrated in the purge gas (argon) for about 15 min prior to each run. For solution samples, stock solutions of enediynes (5.0 mg) in 1,4-CHD (0.5 mL) were prepared and 50 $\mu$L of the stock solutions was sealed in high volume aluminum pans with O-rings in a glovebox under argon.

Conventional DSC was used to determine the reaction kinetics using the ASTM E-698 thermal stability protocol.[23] This protocol is used to determine Arrhenius activation energies and preexponential factors.

**Kinetic Studies. 1,2-Diethynylbenzene (1).** A 10 mL volumetric flask was charged with 1,2-diethynylbenzene (7.1 mg, 5.6 × $10^{-3}$ M), 1,2,3,4-tetraphenylnaphthalene (5.3 mg), and 1,4-cyclohexadiene (0.4 mL, 0.6 M). The solution was analyzed with GC and HPLC to determine the initial concentration of enediynes (5.6 × $10^{-3}$ M). The GC time program had the following parameters: initial temperature = 70 °C for 5 min, 20 °C/min until 220 °C and hold for 5 min, then 30 °C/min until 250 °C and hold for 20 min. Retention times: $t_{ED}$ = 5.5 min, $t_{naphth}$ = 7.0 min, and $t_{std}$ = 28.5 min. The following conditions were used for kinetic analysis using HPLC: A:B 9.5:0.5 solvent system (A = hexanes; B = hexanes/ethyl acetate 100/1), 1 mL/min flow rate, 250 nm detector wavelength. Retention times: $t_{std}$ = 7.7 min and $t_{ED}$ = 23.6 min.

**2,3-Diethynyl-1-methoxybenzene (1)/Trideuteriomethoxybenzene (3).** A 10 mL volumetric flask was charged with 2,3-diethynyl-1-methoxybenzene (**1**) (5.2 mg, 3.3 × $10^{-3}$ M), 1,2,3,4-tetraphenylnaphthalene (5.6 mg), and 1,4-cyclohexadiene (0.3 mL, 0.3 M). The solution was analyzed with GC and HPLC to determine the initial enediyne concentration (3.33 × $10^{-3}$ M). The GC time program had the following parameters: initial temperature = 70 °C for 5 min, 20 °C/min until 220 °C and hold for 5 min, then 30 °C/min until 250 °C and hold for 20 min. Retention times: $t_{ED}$ = 8.8 min, $t_{naphth}$ = 9.4 min, and $t_{std}$ = 28.5 min. The following conditions were used for kinetic analysis using HPLC: A:B 8.5:1.5 solvent system (A = hexanes; B = hexanes/ethyl acetate 120/1), 1 mL/min flow rate, 265 nm detector wavelength. Retention times: $t_{std}$ = 13.0 min and $t_{ED}$ = 41.5 min.

**Kinetic Studies under Different Concentrations of 1,4-Cyclohexadiene. 1,2-Diethynylbenzene (1).** A 10 mL volumetric flask was charged with 1,2-diethynylbenzene (25.0 mg, 19.8 × $10^{-3}$ M) and 1,2,3,4-tetraphenylnaphthalene (25.0 mg). Five master solutions (3.96 × $10^{-3}$ M each) were prepared with different concentrations of 1,4-cyclohexadiene, [1,4-CHD] = 0.04, 0.10, 0.20, 0.40, 0.60, and 0.80 M. The enediynes initial concentration for every stock solution was determined by GC and HPLC as 3.9 × $10^{-3}$ M. Kinetic experiments were performed at 188 °C. The GC time program had the following parameters: initial temperature = 70 °C for 5 min, 20 °C/min until 220 °C and hold for 5 min, then 30 °C/min until 250 °C and hold for 20 min. Retention times: $t_{ED}$ = 5.5 min, $t_{naphth}$ = 7.0 min, and $t_{std}$ = 28.5 min. For kinetic analysis using HPLC the following conditions were used: A:B 9.5:0.5 solvent system (A = hexanes; B = hexanes/ethyl acetate 100/1), 1 mL/min flow rate, 250 nm detector wavelength. Retention times: $t_{std}$ = 7.7 min and $t_{ED}$ = 23.6 min.

**2,3-Diethynyl-1-methoxybenzene (1).** A 10 mL volumetric flask was charged with 2,3-diethynyl-1-methoxybenzene (**1**) (12.5 mg, 8.1 × $10^{-3}$ M) and 1,2,3,4-tetraphenylnaphthalene (25.0 mg). Five master solutions (1.6 × $10^{-3}$ M each) were prepared with different concentrations of 1,4-cyclohexadiene, [1,4-CHD] = 0.00, 0.02, 0.04, 0.08, 0.16, 0.24, 0.32, and 0.40 M. The enediynes initial concentration for every stock solution was determined by GC as 1.4 × $10^{-3}$ M. Kinetic experiments were performed at 170 °C. The GC time program had the following parameters: initial temperature = 70 °C for 5 min, 20 °C/min until 220 °C and hold for 5 min, then 30 °C/min until 250 °C and hold for 20 min. Retention times: $t_{ED}$ = 8.8 min, $t_{naphth}$ = 9.4 min, and $t_{std}$ = 28.5 min.

**Kinetic Studies of 2,3-Diethynyl-1-trideuteriomethoxybenzene (3) in the Absence of 1,4-CHD.** A 10 mL volumetric flask was charged with 2,3-diethynyl-1-trideuteriomethoxybenzene (**3**) (7.8 mg, 8.1 × $10^{-3}$ M) and 1,2,3,4-tetraphenylnaphthalene (7.2 mg). The volumetric flask was filled to the mark with chlorobenzene. The solution was mixed and analyzed with GC to determine their initial enediynes concentration (5.3 × $10^{-3}$ M). Fifteen capillary melting-point tubes were filled with 75 $\mu$L of the solution. The capillary tubes were frozen by liquid nitrogen, degassed under high vacuum, and sealed with only enough space for liquid expansion. The capillary tubes were placed in an oil bath heated at 170 °C and monitored for 2−3 half-lives. The GC time program had the following parameters: initial temperature = 70 °C for 5 min, 20 °C/min until 220 °C and hold for 5 min, then 30 °C/min until 250 °C and hold for 20 min. Retention times: $t_{ED}$ = 8.8 min and $t_{std}$ = 28.5 min.

**Acknowledgment.** The authors are grateful to the National Science Foundation (CHE-0316598) and to the Material Research and Technology (MARTECH) Center at Florida State University for partial support of this research, to the 3M Company for an Untenured Faculty Award, and to Professor Jack Saltiel and Dr. Serguei Kovalenko for helpful discussions. The authors thank Dr. U. Goli and Mr. H. Henricks of the Biochemical Analysis and Synthesis Services laboratory (BASS

(23) Standard Test Method for Arrhenius Kinetic Constants for Thermally Unstable Materials (ANSI/ASTM E698-99). *ASTM Book of Standards*; ASTM: Philadelphia, PA, 1999; pp 299−305.

Lab) and Dr. J. Vaughn, Dr. T. Gedris and Dr. S. Freitag of the NMR facility at the Department of Chemistry and Biochemistry at Florida State University.

**Supporting Information Available:** Additional information including experimental and computational details such as synthesis and characterization details, kinetic procedures and derivation of kinetic equations. This material is available free of charge via the Internet at http://pubs.acs.org.

JO051857N